Inorganic Chemistry

Article

pubs.acs.org/IC

Density Functional Investigation of the Water Oxidation by Iron Complexes Based on Tetradentate Nitrogen Ligands

Esra E. Kasapbasi*,[†] and Myung-Hwan Whangbo*,[‡]

[†]Biomedical Equipment Technology Program, Istanbul Aydin University, Istanbul 34295, Turkey

[‡]Department of Chemistry, North Carolina State University, Raleigh, North Carolina 27695-8204, United States

Supporting Information

ABSTRACT: Recently it was discovered that the iron coordination complex $L^{N4}Fe(II)(OTf)_2$ (**1**) (L^{N4} = neutral tetraazadendate ligand and OTf = OSO_2CF_3) and its analogues are efficient water oxidizing catalysts (WOCs) in aqueous acidic solution with excess amount of ceric(IV) ammonium nitrate (CAN), $[Ce(IV)(NO_3)_6](NH_4)_2$, as sacrificial oxidants. The probable mechanism of water oxidation by these catalysts was explored on the basis of density functional theory (DFT) and time-dependent DFT (TD-DFT) calculations for **1** as a representative WOC. We examined the conversion of **1** to the resting intermediate $[L^{N4}Fe(IV)(O)(OH_2)]^{2+}$ [**2**(IV)] as well as two catalytic cycles involving **2**(IV): one proposed by Fillol et al. [*Nat. Chem.* **2011**, 3, 1] in which the Fe oxidation states of the intermediate species vary from +2 to +5, and the alternative cycle in which they remain constant at +4. In addition, we investigated the role of the sacrificial oxidant CAN in driving the catalytic cycle. Our DFT and TD-DFT calculations confirm the experimental observation that **2**(IV) is the resting species, and indicate that the catalytic cycle in which the Fe oxidation states of the intermediate species remain at +4 is energetically more favorable.

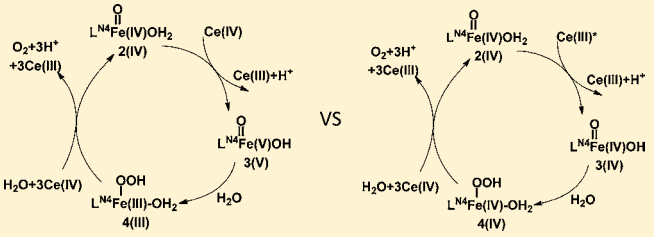

1. INTRODUCTION

In coping with the energy shortage in the near future expected from the depletion of fossil fuels,[1,2] it is a crucial task to search for renewable energy resources based on solar energy. An important goal of extensive research efforts toward such renewable energy resources is to find effective ways of utilizing sunlight energy. Studies of artificial photosynthetic reactions aimed at understanding the factors controlling the water splitting process, $2H_2O \rightarrow 2H_2 + O_2$, have received much attention.[3−11] This uphill-energy reaction (ΔG° = 113 kcal/mol) consists of the H_2 formation and water oxidation processes (eq 1). The water oxidation catalysis requires a multielectron stepwise buildup of high redox potentials and is hence the bottleneck of the water splitting process based on sunlight.

$$4H^+ + 4e^- \rightarrow 2H_2 \quad (1a)$$

$$2H_2O \rightarrow O_2 + 4H^+ + 4e^- \quad (1b)$$

Since the revolutionary work of Fujishima and Honda,[12] numerous photoanodes coupled with various water oxidation catalysts (WOCs) have been designed. Recently, a series of transition-metal substituted polyoxometalate (POM) has been found to be efficient WOCs in homogeneous light-driven water oxidation systems.[13−20] Efficient homogeneous WOCs are mostly based on scarce transition metals. The search for readily available WOCs has recently led Fillol et al.[21] to discover that, in aqueous acidic solution (pH 1) with excess amount of ceric(IV) ammonium nitrate (CAN),[22] $[Ce(IV)(NO_3)_6](NH_4)_2$, as sacrificial oxidants, the iron coordination complexes of the type $L^{N4}Fe(II)(OTf)_2$ (**1**) (L^{N4} = neutral tetraazadendate ligand and OTf = OSO_2CF_3) dissolved in water catalyze homogeneous water oxidation to give O_2 with high efficiency during a period of hours. In view of the potential importance of these iron-based WOCs, it is imperative to investigate the proposed mechanism on the basis of electronic structure calculations. The objective of the present study is to understand the water oxidation mechanism of the WOCs, which we explore on the basis of DFT electronic structure calculations for **1**. We expect that the outcome of our study will enable one to better understand the factors governing the water oxidation by the WOCs and ultimately pave a way to produce more efficient WOCs.

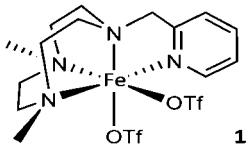

1

2. DETAILS OF CALCULATIONS

To gain insight into the water oxidation catalysis by **1** in an aqueous acidic solution with excess amount of CAN, we carried out DFT[23,24] electronic structure calculations using the

Received: June 22, 2012
Published: October 1, 2012

dx.doi.org/10.1021/ic3013359 | *Inorg. Chem.* 2012, 51, 10850−10855

B3LYP[25] functional. For the ground state structures of some reaction intermediates to be discussed below, we optimized their structures with the 6-31G(d)[26] basis set and then we calculated single point energy with higher basis set 6-311+G(d,p).[27,28] For the Ce atom in CAN and its related species, we employed the Stuttgart RSC Segmented/ECP[29] basis set. The UV−vis excitation spectra for the ground-state structures of the intermediate $[L^{N4}Fe(IV)(O)(OH_2)]^{2+}$, **2**(IV), and its reduced species, $[L^{N4}Fe(III)(O)(OH_2)]^{+}$, **2**(III), and $[L^{N4}Fe(II)(O)(OH_2)]^{0}$, **2**(II), were calculated and the energies of the 20 lowest-excited states were found by performing TD-DFT[30,31] calculations with the 6-31G(d) basis set. For the geometry optimization and the excitation spectrum calculations of a molecular species, the solvent effect was taken into consideration by using the conductor polarizable continuum model (CPCM).[32] DFT calculations were carried out using the Gaussian09 program package.[33]

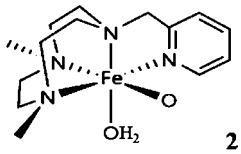

2

In our use of the structure numbers designating various molecular species, the oxidation states of their transition-metal or rare-earth ions are given in parentheses. Thus, for example, **2**(III) and **2**(II) have the same molecular formula but differ in the number of electrons; namely, **2**(III) and **2**(II) have one and two more electrons than does **2**(IV), respectively. It should also be pointed out that, in balancing the various equilibriums concerning the addition/subtraction of protons and electrons, we use the sacrificial oxidants CAN in aqueous solution (see below).

In what follows, spin-polarized DFT calculations were performed to optimize the structures of all molecular species including those related to CAN, i.e., $[Ce(IV)(NO_3)_6]^{2-}$, **9**(IV); $[Ce(III)(NO_3)_6]^{3-}$, **9**(III); and $[Ce(III)(NO_3)_5]^{2-}$, **10**(III), were also optimized. The energies of the various molecular species calculated with 6-31G (d) and 6-311+G (d,p) basis sets are given in Table S1 of Supporting Information (SI) and the enthalpy changes of the various reaction paths described in the following in Table S2 of SI.

3. FEASIBILITY OF FILLOL ET AL.'S MECHANISM

To explain their experimental observations, Fillol et al.[21] proposed the catalysis mechanism summarized in Figure 1. The WOC **1** is initially converted to the intermediate **2**(IV), which subsequently becomes $[L^{N4}Fe(V)(O)(OH)]^{2+}$, **3**(V). Upon adding H_2O, the latter is converted to $[L^{N4}Fe(III)(OOH)(OH_2)]^{2+}$, **4**(III), which then interacts with water and Ce(IV) ions to produce O_2 and regenerate the intermediate **2**(IV). In this catalytic cycle, **2**(IV) → **3**(V) → **4**(III) → **2**(IV), the intermediate **2**(IV) is the only one identified experimentally, and the rate-determining step of the catalytic cycle is the conversion from **2**(IV) to **3**(V) according to the kinetic study of Fillol et al. At present the energetics involved in each step of the catalytic cycle is unknown. In this section, we evaluate the feasibility of Fillol et al.'s mechanism by calculating the enthalpy of each reaction step of the catalytic cycle on the basis of DFT calculations.

3.1. Formation of 2(IV) from 1. Let us first examine how the intermediate **2**(IV) might be generated from the WOC **1**.

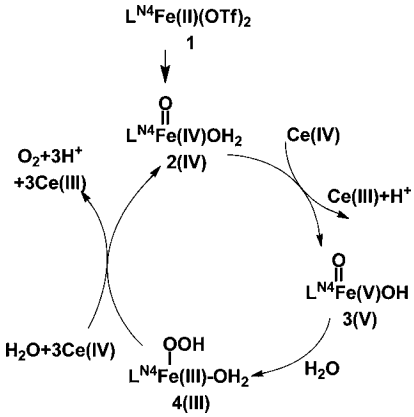

Figure 1. Fillol et al.'s mechanism of the water oxidation catalysis by $L^{N4}Fe(II)(OTf)_2$ (**1**) (ref 21).

$$\mathbf{1} + 2H_2O \rightarrow \mathbf{2}(IV) + 2TfO^- + 2H^+ + 2e^- \quad \Delta H_1 \qquad (2)$$

It is possible that the oxidation of **1** may produce **2**(II) and **2**(III) on the way to **2**(IV). To see if such reduced species of **2**(IV) can also be involved in the catalytic cycle of the water oxidation, we first examine the relative stabilities of **2**(II), **2**(III), and **2**(IV). Our calculations reveal that the ground states of **2**(II), **2**(III), and **2**(IV) are $S = 0$, $S = {}^1/_2$, and $S = 1$ species, respectively. The Fe-environments in **2**(II), **2**(III), and **2**(IV) are distorted octahedral such that their t_{2g}-block levels are split into 1a < 2a ≪ 3a as depicted in Figure 2. Thus, the d-block

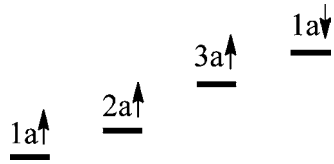

Figure 2. Split pattern of the occupied t_{2g}-block levels of **2**(IV) from the spin-polarized DFT calculations.

electron configurations of **2**(II), **2**(III), and **2**(IV) are given by $(1a)^2(2a)^2(3a)^2$, $(1a)^2(2a)^2(3a)^1$, and $(1a)^2(2a)^1(3a)^1$, respectively, thereby leading to the $S = 0$, $S = {}^1/_2$, and $S = 1$ species, respectively. Our DFT calculations indicate that **2**(IV) is considerably less stable than its reduced species **2**(II) and **2**(III).

$$\mathbf{2}(II) \rightarrow \mathbf{2}(III) + e^- \quad \Delta H_2 = 70.7 \text{ kcal/mol} \qquad (3a)$$

$$\mathbf{2}(III) \rightarrow \mathbf{2}(IV) + e^- \quad \Delta H_3 = 153.3 \text{ kcal/mol} \qquad (3b)$$

At this point, therefore, it is not possible to exclude the possibility that **2**(II) and **2**(III) are also involved in the catalytic cycle of the water oxidation.

Fillol et al. observed the intermediate **2**(IV), i.e., a Fe(IV)═O complex, by UV−vis spectroscopy measurements.[21] The UV−vis spectrum of **2**(IV) is very similar to those of other nonheme Fe(IV)═O complexes.[10a,11b,c] To confirm Fillol et al.'s observation, we calculate the absorption spectra of **2**(II), **2**(III), and **2**(IV) by TD-DFT calculations. The resulting spectra are compared in Figure 3, which shows that **2**(II) with $S = 0$ ion Fe(II) has excitation primarily below 450 nm. This is understandable because the optical excitation, being the ligand-to-metal change transfer in nature, must involve the empty e_g-block levels that lie considerably higher in energy. Compound **2**(III) with $S = {}^1/_2$ ion Fe(III) has excitation primarily below

dx.doi.org/10.1021/ic3013359 | Inorg. Chem. 2012, 51, 10850−10855

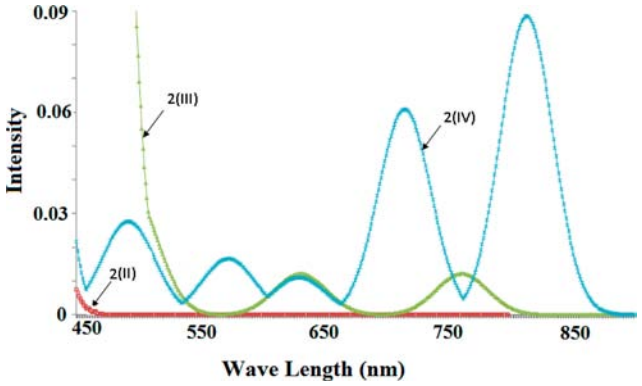

Figure 3. Excitation spectra of $[L^{N4}Fe(II)(O)(OH_2)]^0$ [**2**(II)], $[L^{N4}Fe(III)(O)(OH_2)]^+$ [**2**(III)], and $[L^{N4}Fe(IV)(O)(OH_2)]^{2+}$ [**2**(IV)] obtained from TD-DFT calculations.

550 nm with very weak excitations around 630 and 770 nm, which results from the fact that now the one empty t_{2g}-block level (i.e., 3a) can participate in the optical excitation. Compound **2**(IV) with $S = 1$ ion Fe(IV) has strong excitations around 720 and 820 nm, weak excitations around 490, 580, and 630 nm, and strong absorption below 450 nm (though not shown in Figure 3). This is due to the participation of the two empty t_{2g}-block levels (i.e., 2a and 3a) in the excitation. Among **2**(II), **2**(III), and **2**(IV), the UV–vis spectrum calculated for **2**(IV) is the only one that is consistent with the experimentally observed spectrum of **2** reported in ref 21; the experimental UV–vis spectrum shows a peak around 776 nm, which is related most likely to the strong excitation peaks around 720 and 820 nm calculated for **2**(IV). This confirms Fillol et al.'s identification of the intermediate **2**(IV) by UV–vis spectroscopy measurements.

The above discussion reveals that **2**(IV) is less stable than **2**(II) and **2**(III), but is produced from **1** in the highly acidic solution of CAN. The energetics involved in the formation of **2**(II), **2**(III), and **2**(IV) from **1** may be discussed by considering the enthalpies calculated for the following reactions:

$$\mathbf{1} + 2H^+ \rightarrow [L^{N4}Fe(II)]^{2+}[\mathbf{8}(II)] + 2HOTf$$
$$\Delta H_4 = 24.1 \text{ kcal/mol} \quad (4a)$$

$$\mathbf{8}(II) + 2H_2O \rightarrow [L^{N4}Fe(II)(OH_2)_2]^{2+}[\mathbf{7}(II)]$$
$$\Delta H_5 = -3.9 \text{ kcal/mol} \quad (4b)$$

$$\mathbf{7}(II) \rightarrow [L^{N4}Fe(IV)(OH_2)_2]^{4+}[\mathbf{7}(IV)] + 2e^-$$
$$\Delta H_6 = 357.0 \text{ kcal/mol} \quad (4c)$$

$$\mathbf{7}(IV) \rightarrow [\mathbf{2}(IV)] + 2H^+ \quad \Delta H_7 = 447.3 \text{ kcal/mol} \quad (4d)$$

The overall reaction of the above four steps is equivalent to eq 2, for which the enthalpy change is $\Delta H_1 = 824.6$ kcal/mol. This is a highly endothermic reaction. Therefore, the thermodynamic driving force enabling the above reaction to take place should be supplied by the energy gain resulting from the reduction of the sacrificial oxidants CAN. Namely, the **9**(IV) part of CAN is reduced to form the anion **9**(III)

$$\mathbf{9}(IV) + e^- \rightarrow \mathbf{9}(III) \quad \Delta H_8 = 111.6 \text{ kcal/mol} \quad (5a)$$

which subsequently becomes protonated to form **10**(III) and HNO_3, namely

$$\mathbf{9}(III) + H^+ \rightarrow \mathbf{10}(III) + HNO_3$$
$$\Delta H_9 = -575.2 \text{ kcal/mol} \quad (5b)$$

Consequently, for the reaction

$$\mathbf{9}(IV) + H^+ + e^- \rightarrow \mathbf{10}(III) + HNO_3$$
$$\Delta H_{10} = -463.6 \text{ kcal/mol} \quad (5c)$$

The energy gain arising from the above reaction is due largely to the protonation of a nitrate anion NO_3^-

$$NO_3^- + H^+ \rightarrow HNO_3 \quad \Delta H_{11} = -270 \text{ kcal/mol} \quad (5d)$$

which is calculated to be strongly exothermic. We now combine eqs 2 and 5c to obtain

$$\mathbf{1} + 2[Ce(IV)(NO_3)_6]^{2-}[\mathbf{9}(IV)] + 2H_2O$$
$$\rightarrow \mathbf{2}(IV) + 2TfO^- + 2[Ce(III)(NO_3)_5]^{2-}[\mathbf{10}(III)]$$
$$+ 2HNO_3 \quad \Delta H_{12} = -102.6 \text{ kcal/mol} \quad (6)$$

Namely, the oxidation of **1** into **2**(IV) is accompanied by the reduction of **9**(IV) to **10**(III), which makes the overall reaction exothermic. At this point we note that the oxidation of **1** takes place in excess amount of CAN. Further, as discussed above, the reduction of CAN is highly exothermic. Consequently, the intermediates **2**(II) and **2**(III) would be readily oxidized to give **2**(IV).

3.2. Oxidation of 2(IV). In Fillol et al.'s mechanism, the intermediate **2**(IV) loses an electron as well as a proton to form the intermediate **3**(V)

$$\mathbf{2}(IV) \rightarrow \mathbf{3}(V) + H^+ + e^- \quad \Delta H_{13} = 388.6 \text{ kcal/mol} \quad (7a)$$

Our calculations show the above reaction to be strongly endothermic because losing a bound electron and deprotonation of water require a considerable amount of energy. As expected, the removal of a proton from **2**(IV) leading to an alternative intermediate $[L^{N4}Fe(IV)(O)(OH)]^+$, **3**(IV)

$$\mathbf{2}(IV) \rightarrow \mathbf{3}(IV) + H^+ \quad \Delta H_{14} = 276.8 \text{ kcal/mol} \quad (7b)$$

is calculated to be considerably less endothermic than the removal of an electron and a proton from **2**(IV) by 112.2 kcal/mol.

The **2**(IV) → **3**(V) conversion requires the coupling of eq 7a with the removal of an electron and a proton by CAN, eq 5c, leading to the combined reaction

$$\mathbf{2}(IV) + \mathbf{9}(IV) \rightarrow \mathbf{3}(V) + \mathbf{10}(III) + HNO_3$$
$$\Delta H_{15} = -75.0 \text{ kcal/mol} \quad (8a)$$

The **2**(IV) → **3**(IV) conversion requires the coupling of eq 7b with the protonation of the **9**(III), eq 5b, leading to the combined reaction

$$\mathbf{2}(IV) + \mathbf{9}(III) \rightarrow \mathbf{3}(IV) + \mathbf{10}(III) + HNO_3$$
$$\Delta H_{16} = -298.4 \text{ kcal/mol} \quad (8b)$$

According to these results, the **2**(IV) → **3**(IV) conversion is more exothermic than the **2**(IV) → **3**(V) conversion by 223.4 kcal/mol. Therefore, in discussing the mechanism of the water

dx.doi.org/10.1021/ic3013359 | Inorg. Chem. 2012, 51, 10850–10855

oxidation, it is necessary to examine the possibility that the **2**(IV) → **3**(IV) conversion, rather than the **2**(IV) → **3**(V) conversion, is the first step of the catalytic cycle. This question is investigated further in the next section.

4. COMPARISON OF THE MECHANISMS INVOLVING 3(IV) AND 3(V)

In this section we probe the elementary reactions that are associated with the intermediate **3**(IV) and **3**(V) in producing O_2 and regenerating the intermediate **2**(IV). The alternative reaction mechanism involving **3**(IV) is proposed in Figure 4. As

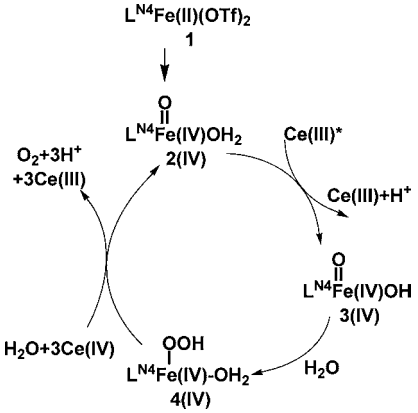

Figure 4. Alternative mechanism of the water oxidation catalysis by $L^{N4}Fe(II)(OTf)_2$ (**1**). Elementary reactions associated with the **2**(IV) → **4**(IV) conversion, where Ce(III)* refers to the $[Ce(III)(NO_3)_6]^{3-}$ ion [i.e., **9**(III)]. **3**(IV) refers to the species resulting from **3**(V) of Figure 1 by adding one electron, and **4**(**IV**) to that resulting from **4**(III) of Figure 1 by removing one electron.

to how the intermediate **4**(III) interacts with water and Ce(IV) ions to produce O_2 and the intermediate **2**(IV), we propose the series of reactions depicted in Figure 5. The corresponding

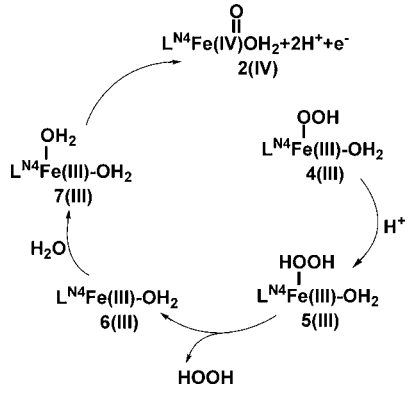

Figure 5. Elementary reactions expected for the **4**(III)→ **2**(IV) conversions in the water oxidation mechanism proposed by Fillol et al.

reactions starting from the intermediate $[L^{N4}Fe(IV)(OOH)(OH_2)]^{3+}$, **4**(IV), are presented in Figure 6. Compound **3**(V) accepts one H_2O to form the intermediate **4**(III). Similarly, **3**(IV) accepts one H_2O to form **4**(IV).

$$\mathbf{3}(V) + H_2O \rightarrow \mathbf{4}(III) \quad \Delta H_{17} = -5.2 \text{ kcal/mol} \tag{9a}$$

$$\mathbf{3}(IV) + H_2O \rightarrow \mathbf{4}(IV) + 2e^- \quad \Delta H_{18} = 278.4 \text{ kcal/mol} \tag{9b}$$

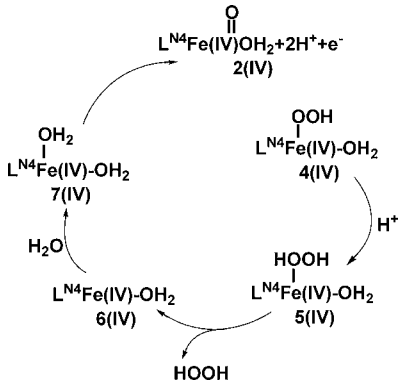

Figure 6. Elementary reactions associated with the **4**(IV) → **2**(IV) conversions.

The **3**(IV) → **4**(IV) conversion requires the combination of eq 9b with the two-electron removal by CAN, eq 5c, leading to the combined reaction

$$\mathbf{3}(IV) + 2[Ce(IV)(NO_3)_6]^{2-}[\mathbf{9}(IV)] + H_2O + 2H^+ \rightarrow \mathbf{4}(IV) + 2[Ce(III)(NO_3)_5]^{2-}[\mathbf{10}(III)] + 2HNO_3 \quad \Delta H_{19} = -648.7 \text{ kcal/mol} \tag{9c}$$

Thus, the **3**(IV) → **4**(IV) conversion is more strongly exothermic than the **3**(V) → **4**(III) conversion, namely, ΔH [**3**(IV) → **4**(IV)] = −648.7 kcal/mol versus ΔH [**3**(V) → **4**(III)] = −5.2 kcal/mol.

For the formation of **2**(IV) from **4**(III), one can suppose the following series of reactions:

$$\mathbf{4}(III) + H^+ \rightarrow [L^{N4}Fe(III)(HOOH)(OH_2)]^{3+}[\mathbf{5}(III)] \quad \Delta H_{20} = -241.7 \text{ kcal/mol} \tag{10a}$$

$$\mathbf{5}(III) \rightarrow [L^{N4}Fe(III)(OH_2)]^{3+}[\mathbf{6}(III)] + HOOH \quad \Delta H_{21} = 14.7 \text{ kcal/mol} \tag{10b}$$

$$\mathbf{6}(III) + H_2O \rightarrow [L^{N4}Fe(III)(OH_2)_2]^{4+}[\mathbf{7}(III)] \quad \Delta H_{22} = 125.9 \text{ kcal/mol} \tag{10c}$$

$$\mathbf{7}(III) + 2[Ce(IV)(NO_3^-)_6]^{2-}[\mathbf{9}(IV)] \rightarrow \mathbf{2}(IV) + 2HNO_3 + 2[Ce(III)(NO_3^-)_5]^{2-}[\mathbf{10}(III)] \quad \Delta H_{23} = -373.3 \text{ kcal/mol} \tag{10d}$$

Thus, the enthalpy change follows for the **4**(III) → **2**(IV) conversion: ΔH [**4**(III)→**2**(IV)] = −474.4 kcal/mol. The formation of **2**(IV) from **4**(IV) can be achieved by the following series of reactions:

$$\mathbf{4}(IV) + H^+ \rightarrow [L^{N4}Fe(IV)(HOOH)(OH_2)]^{4+}[\mathbf{5}(IV)] \quad \Delta H_{24} = -186.3 \text{ kcal/mol} \tag{11a}$$

$$\mathbf{5}(IV) \rightarrow [L^{N4}Fe(IV)(OH_2)]^{4+}[\mathbf{6}(IV)] + HOOH \quad \Delta H_{25} = -341.7 \text{ kcal/mol} \tag{11b}$$

$$\mathbf{6}(IV) + H_2O \rightarrow \mathbf{7}(IV) \quad \Delta H_{26} = 2.7 \text{ kcal/mol} \tag{11c}$$

dx.doi.org/10.1021/ic3013359 | Inorg. Chem. 2012, 51, 10850−10855

$$7(\mathrm{IV}) + 2NO_3^- \rightarrow 2(\mathrm{IV}) + 2HNO_3$$

$$\Delta H_{27} = -92.7 \text{ kcal/mol} \quad (11d)$$

Thus, the enthalpy change follows for the 4(IV) → 2(IV) conversion: ΔH [4(IV)→2(IV)] = −259.2 kcal/mol. (The optimized structures of the intermediates 5(III) and 5(IV) determined from our DFT calculations are given in Figure S1 of SI).

Consequently, the enthalpy change for the 3(V) → 2(IV) conversion, ΔH [3(V)→2(IV)] = −479.6 kcal/mol, is less strongly exothermic than that for the 3(IV) → 2(IV) conversion, ΔH [3(IV)→2(IV)] = −907.9 kcal/mol. Furthermore, we note that the 2(IV) → 3(IV) conversion is more exothermic than the 2(IV) → 3(V) conversion by 223.4 kcal/mol. As a consequence, the catalytic cycle involving the intermediate 3(IV) is energetically more favorable than that involving the intermediate 3(V).

Finally, we note that O_2 is produced by the oxidation of HOOH with CAN (see eq 5).

$$HOOH \rightarrow O_2 + 2H^+ + 2e^- \quad \Delta H_{28} = 68.8 \text{ kcal/mol} \quad (12)$$

Although this reaction is endothermic, it does not present any problem because the other reactions of the catalytic cycle are strongly exothermic.

5. CONCLUSION

In the present DFT/TD-DFT study we examined the mechanism of water oxidation associated with the WOC 1 in strongly acidic solution of CAN. Our calculations confirm the conversion of 1 into 2(IV) observed by Fillol et al. The Fe atom of 2(IV) exists as an S = 1 ion Fe(IV) because the d-electrons are accommodated in the t_{2g}-block levels. For the catalytic cycle, Fillol et al. proposed the sequence of reactions that involve 2(IV) → 3(V) → 4(II) → 5(II) → 6(II) → 7(II) → 2(IV). As an alternative catalytic cycle, we proposed the sequence 2(IV) → 3(IV) → 4(IV) → 5(IV) → 6(IV) → 7(IV) → 2(IV) in which all intermediates contain S = 1 ions Fe(IV). Our calculations indicate that the alternative mechanism is energetically more favorable. It would be of interest to experimentally determine which mechanism, Fillol et al.'s or its alternative proposed in the present work, is more appropriate for the water oxidation associated with the WOC 1 in strongly acidic solution of CAN. An interesting implication of our study is that other 3d transition metal ions of d^4 electron count generating an S = 1 electron configuration in an octahedral environment might lead to efficient water oxidation catalysis. Finally, we note that, in understanding the energetics of a catalytic oxidation reaction, it is crucial to examine the energetics associated with its sacrificial oxidant on an equal footing.

■ ASSOCIATED CONTENT

Supporting Information

Figure S1 as well as Tables S1 and S2. This material is available free of charge via the Internet at http://pubs.acs.org.

■ AUTHOR INFORMATION

Corresponding Author

*E-mail: eminekasapbasi@aydin.edu.tr (E.E.K.), mike_whangbo@ncsu.edu (M.-H.W.).

Notes

The authors declare no competing financial interest.

■ ACKNOWLEDGMENTS

Our DFT calculations have used the computing resources of the High Performance and Grid Computing Center at NCSU (http://www.ncsu.edu/itd/hpc/main.php).

■ REFERENCES

(1) U.S. Energy Information Administration. *International Energy Outlook*; DOE/EIA-0484 (Office of Integrated Analysis and Forecasting, U.S. Department of Energy).
(2) Lewis, N. S. *Energy and Transportation*; The National Academies Press: Washington, DC, 2003; pp 33−39.
(3) (a) Meyer, T. J. *Acc. Chem. Res.* **1989**, *22*, 163. (b) Alstrum-Acevedo, J. H.; Brennaman, M. K.; Meyer, T. J. *Inorg. Chem.* **2005**, *44*, 6802.
(4) (a) Eisenberg, R.; Nocera, D. G. *Inorg. Chem.* **2005**, *44*, 6799. (b) Dempsey, J. L.; Esswein, A. J.; Manke, D. R.; Rosenthal, J.; Soper, J. D.; Nocera, D. G. *Inorg. Chem.* **2005**, *44*, 6879.
(5) Yano, J.; Kern, J.; Sauer, K.; Latimer, M. J.; Pushkar, Y.; Biesiadka, J.; Loll, B.; Saenger, W.; Messinger, J.; Zouni, A.; Yachandra, V. K. *Science* **2006**, *314*, 821.
(6) Tong, L.; Duan, L.; Xu, Y.; Privalov, T. *Angew. Chem., Int. Ed.* **2011**, *50*, 445.
(7) McDaniel, N. D.; Coughlin, F. J.; Tinker, L. L.; Bernhard, S. *J. Am. Chem. Soc.* **2008**, *130*, 210.
(8) Lalrempuia, R.; McDaniel, N. D.; Müller-Bunz, H.; Bernhard, S.; Albrecht, M. *Angew. Chem., Int. Ed.* **2010**, *49*, 9765.
(9) Hull, J. F.; Balcells, D.; Blakemore, J. D.; Incarvito, C. D.; Eisenstein, O.; Brudvig, G. W.; Crabtree, R. H. *J. Am. Chem. Soc.* **2009**, *131*, 8730.
(10) (a) Rohde, J.-W.; In, J.-H.; Lim, M. H.; Brennessel, W. W.; Bukowski, M. R.; Stubna, A.; Münck, E.; Nam, W. W.; Que, L., Jr. *Science* **2003**, *299*, 1037. (b) Rohde, J.-W.; Torelli, S.; Shan, X. P.; Lim, M. H.; Klinker, E. J.; Kaizer, J.; Chen, C.; Nam, W. W.; Que, L., Jr. *J. Am. Chem. Soc.* **2004**, *16*, 16750.
(11) (a) Nam, W. W. *Acc. Chem. Res.* **2007**, *40*, 522. (b) Lee, Y.-M.; Kotani, H.; Suenobu, T.; Nam, W. W.; Fukuzumi, S. *J. Am. Chem. Soc.* **2008**, *130*, 434. (c) Lee, Y.-M.; Dhuri, S. N.; Sawant, S. C.; Cho, J. H.; Kubo, M.; Ogura, T.; Fukuzumi, S.; Nam, W. W. *Angew. Chem.* **2009**, *121*, 1835.
(12) Fujishima, A.; Honda, K. *Nature* **1972**, *238*, 37.
(13) Geletii, Y. V.; Huang, Z. Q.; Hou, Y.; Musaev, G.; Lian, T. Q.; Hill, C. L. *J. Am. Chem. Soc.* **2009**, *131*, 7522.
(14) Besson, C.; Huang, Z. Q.; Geletii, Y. V.; Lense, S.; Hardcastle, K. I.; Musaev, D. G.; Lian, T. Q.; Proust, A.; Hill, C. L. *Chem. Commun.* **2010**, *46*, 2784.
(15) Geletii, Y. V.; Yin, Q. S.; Hou, Y.; Huang, Z. Q.; Ma, H. Y.; Song, J.; Besson, C.; Luo, Z.; Cao, R.; O'Halloran, K. P.; Zhu, G. B.; Zhao, C. C.; Vickers, J. W.; Ding, Y.; Mohebbi, S.; Kuznetsov, A. E.; Musaev, D. G.; Lian, T. Q.; Hill, C. L. *Isr. J. Chem.* **2011**, *51*, 238.
(16) Huang, Z. Q.; Luo, Z.; Geletii, Y. V.; Vickers, J. W.; Yin, Q. S.; Wu, D.; Hou, Y.; Ding, Y.; Song, J.; Musaev, D. G.; Hill, C. L.; Lian, T. Q. *J. Am. Chem. Soc.* **2011**, *133*, 2068.
(17) Puntoriero, F.; La Ganga, G.; Sartorel, A.; Carraro, M.; Scorrano, G.; Bonchio, M.; Campagna, S. *Chem. Commun.* **2010**, *46*, 4725.
(18) Huang, Z.; Geletii, Y. V.; Wu, D.; Anfuso, C. L.; Musaev, D. G.; Hill, C. L.; Lian, T. *Proc. SPIE* **2011**, *8109*, 810903.
(19) Hill, C. L. *J. Mol. Catal. A: Chem.* **2007**, *262*, 2.
(20) Han, Z.; Bond, A. M.; Zhao, C. *Sci. China: Chem.* **2011**, *54*, 1877.
(21) Fillol, J. L.; Codola, Z.; Garcia-Bosch, I.; Gómez, L.; Pla, J. J.; Costas, M. *Nat. Chem.* **2011**, *3*, 807.
(22) Beineke, T. A.; Delgaudio, J. *Inorg. Chem.* **1968**, *7*, 715.
(23) Stephens, P. J.; Devlin, F. J.; Chabalowski, C. F.; Frisch, M. J. *J. Phys. Chem.* **1994**, *98*, 11623.

(24) Stephens, P. J.; Devlin, F. J.; Ashvar, C. S.; Bak, K. L.; Taylor, P. R.; Frisch, M. J. *ACS Symp. Ser.* **1996**, *629*, 105.
(25) Becke, A. D. *J. Chem. Phys.* **1993**, *98*, 5648.
(26) Ditchfield, R.; Hehre, W. J.; Pople, J. A. *J. Chem. Phys.* **1971**, *54*, 724.
(27) Petersson, G. A.; Bennett, A.; Tensfeldt, T. G.; Al-Laham, M. A.; Shirley, W. A. *J. Chem. Phys.* **1988**, *89*, 2193.
(28) Petersson, G. A.; Al-Laham, M. A. *J. Chem. Phys.* **1991**, *94*, 6081.
(29) Schuchardt, K. L.; Didier, B. T.; Elsethagen, T.; Sun, L.; Gurumoorthi, V.; Chase, J.; Li, J.; Windus, T. L. *J. Chem. Inf. Model.* **2007**, *47* (3), 1045.
(30) De Backer, M.; Hureau, M.; Depriester, M.; Deletoille, A.; Sargent, A. L.; Forshee, P. B.; Sibert, J. W. *J. Electroanal. Chem.* **2008**, *612*, 97.
(31) Homem-de-Mello, P.; Mennucci, B.; Tomasi, J.; da Silva, A. B. F. *Theor. Chem. Acc.* **2005**, *113*, 274.
(32) Barone, V.; Cossi, M. J. *Phys. Chem. A* **1998**, *102*, 1995.
(33) Frisch, M. J.; Trucks, G. W.; Schlegel, H. B.; Scuseria, G. E.; Robb, M. A.; Cheeseman, J. R.; Scalmani, G.; Barone, V.; Mennucci, B.; Petersson, G. A.; Nakatsuji, H.; Caricato, M.; Li, X.; Hratchian, H. P.; Izmaylov, A. F.; Bloino, J.; Zheng, G.; Sonnenberg, J. L.; Hada, M.; Ehara, M.; Toyota, K.; Fukuda, R.; Hasegawa, J.; Ishida, M.; Nakajima, T.; Honda, Y.; Kitao, O.; Nakai, H.; Vreven, T.; Montgomery, J. A., Jr.; Peralta, J. E.; Ogliaro, F.; Bearpark, M.; Heyd, J. J.; Brothers, E.; Kudin, K. N.; Staroverov, V. N.; Kobayashi, R.; Normand, J.; Raghavachari, K.; Rendell, A.; Burant, J. C.; Iyengar, S. S.; Tomasi, J.; Cossi, M.; Rega, N.; Millam, J. M.; Klene, M.; Knox, J. E.; Cross, J. B.; Bakken, V.; Adamo, C.; Jaramillo, J.; Gomperts, R.; Stratmann, R. E.; Yazyev, O.; Austin, A. J.; Cammi, R.; Pomelli, C.; Ochterski, J. W.; Martin, R. L.; Morokuma, K.; Zakrzewski, V. G.; Voth, G. A.; Salvador, P.; Dannenberg, J. J.; Dapprich, S.; Daniels, A. D.; Farkas, O.; Foresman, J. B.; Ortiz, J. V.; Cioslowski, J.; Fox, D. J. *Gaussian 09, revision A.02*; Gaussian, Inc.: Wallingford, CT, 2009.